Pt-Mn-Al trimetallic nanoporous catalyst for reversible hydrogenation/oxidative dehydrogenation of *N*-heterocycles

Yunpeng Wang, [+a] *Ziyi Zhang,* [+b] *Shize Wang,*[a] *Qiang Xu,*[c] *Xiujuan Feng,*[a,*] *Yanhui Li,*[d] *Xuan Zhang,*[a] *Yoshinori Yamamoto,*[e] *Ming Bao* [a,*]

[a] State Key Laboratory of Fine Chemicals, Frontier Science Center for Smart Materials, Dalian University of Technology, Dalian 116024, China.

[b] Key Laboratory of Industrial Ecology and Environmental Engineering (Ministry of Education), School of Environmental Science and Technology, Dalian University of Technology, Dalian 116024, China.

[c] Instrumental Analysis Center, Dalian University of Technology, Dalian 116024, China.

[d] School of Materials Science and Engineering, Dalian University of Technology, Dalian 116024, China.

[e] Research Organization of Science and Technology, Ritsumeikan University, Kusatsu, Shiga 525-8577, Japan.

[+] Yunpeng Wang and Ziyi Zhang contributed equally to this work.

Email address of the corresponding author: fengxiujuan@dlut.edu.cn, mingbao@dlut.edu.cn.

Table of contents

Contents

1 General information

^1H and ^{13}C NMR spectra were recorded on a Bruker Avance II-400 spectrometer (400 MHz for ^1H, 100 MHz for ^{13}C); $CDCl_3$ was used as a solvent, while TMS was used as an internal standard. The chemical shifts are reported in ppm downfield (δ) from TMS, the coupling constants J are given in Hz. The residual solvent peak was used as an internal reference: proton (chloroform δ 7.26), carbon (chloroform δ 77.1). The peak patterns are indicated as follows: s, singlet; d, doublet; t, triplet; q, quartet; m, multiplet; br, broad. TLC was carried out on SiO_2 (silica gel 60 F254, Merck), and the spots were located with UV light. Flash chromatography was carried out on SiO_2 (silica gel 60, 200-300 meth). The H_2-temperature programmed desorption (H-TPD) study was performed by CHEMBET-3000, 0.05 g catalyst was reduced with H_2 at 400 °C for 2 h, and then cooled to 30 °C and exposed to H_2 flow for 40 min. Thereafter, the sample was flushed with He for 40 min to remove physically adsorbed hydrogen, the TPD of H_2 was monitored while raising the catalysts temperature at a rate of 10 °C/min from 50 °C to 850 °C. O_2-temperature programmed desorption (O-TPD) of the catalyst was performed by CHEMBET-3000, 0.05 g catalyst was pretreated with He at 300 °C for 1 h, and then cooled to 30 °C and exposed to 5% O_2/He flow for 1 h. Thereafter, the sample was flushed with He for 40 min to remove physically adsorbed oxygen, the TPD of O_2 was monitored while raising the catalysts temperature at a rate of 10 °C/min from 50 °C to 900 °C. In the test of CO titration, the catalyst was reduced with H_2 at 400 °C for 2 h, then purged with He for 30 min and cooled to 30 °C, the CO adsorption capacity was obtained by 5 pluses to saturate the total surface of the catalysts. The TOF value was calculated with the following equation:

$$TOF\ (h^{-1}) = \frac{n_{quinoline}(mol)}{n_{Pt}(mol) \times dispersion \times time(h)}$$

where $n_{quinoline}$ is the converted moles of quinoline, n_{Pt} is determined from the Pt content obtained by ICP-MS, the dispersion of active species (0.5%) was measured by CO titration.

2 Leaching studies of the PtMnAlNPore catalyst

To study the mechanism of the PtMnAlNPore catalyzed hydrogenation of quinolines. Leaching tests were performed to determine whether the reaction occurred heterogeneously on the surface of PtMnAlNPore catalyst or homogeneously through dissolved Pt species (Scheme 1). After the reaction proceeded under the standard conditions for 6 h, half of the supernatant was transferred into another reaction vessel, and the yield of **2a** was determined to be 30%. The yield of **2a** did not change when half the supernatant was continuously stirred under 0.3 MPa H_2 in the absence of PtMnAlNPore catalyst for 6 h. Conversely, the yield of **2a** reached 92% in the reaction of the residual mixture containing PtMnAlNPore catalyst after 6 h (Scheme 1). Moreover, inductively coupled plasma-mass spectrometry (ICP-MS) was used to determine the Pt species leaching. As predicted, no metal ion leached from the PtMnAlNPore catalyst. These results clearly indicated that the hydrogenation reaction proceeded through a heterogeneous process.

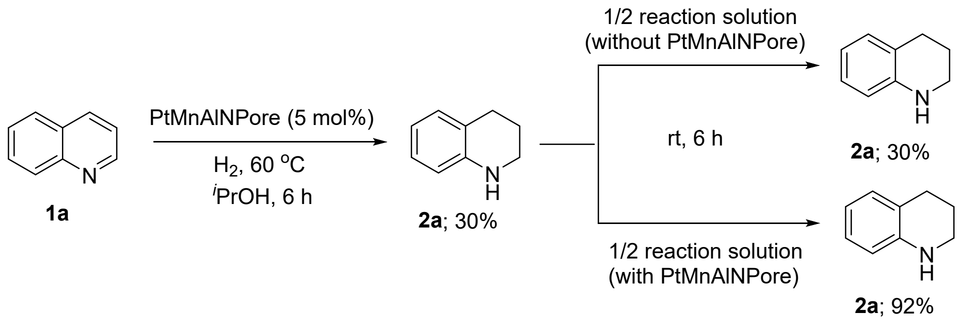

Scheme 1. Leaching test of the PtMnAlNPore-catalyzed selective hydrogenation of quinolines.

3 Characterization of catalyst

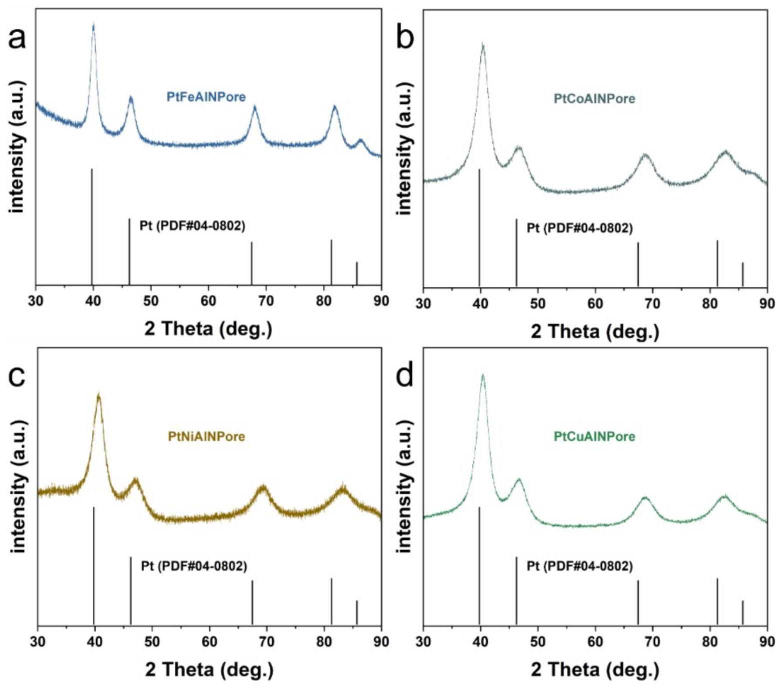

Figure 1. XRD pattern of (a) PtFeAlNPore, (b) PtCoAlNPore, (c) PtNiAlNPore, (d) PtCuAlNPore.

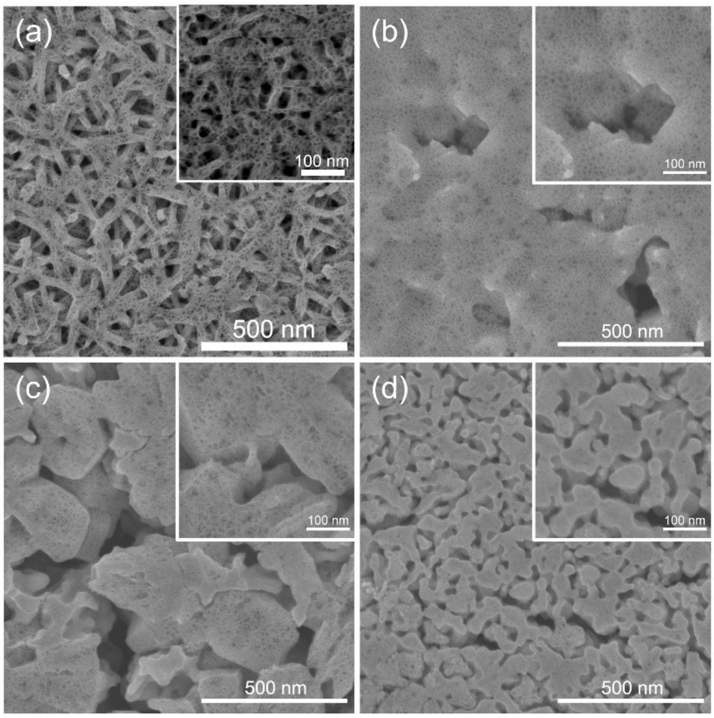

Figure 2. SEM image of (a) PtFeAlNPore, (b) PtCoAlNPore, (c) PtNiAlNPore, (d) PtCuAlNPore.

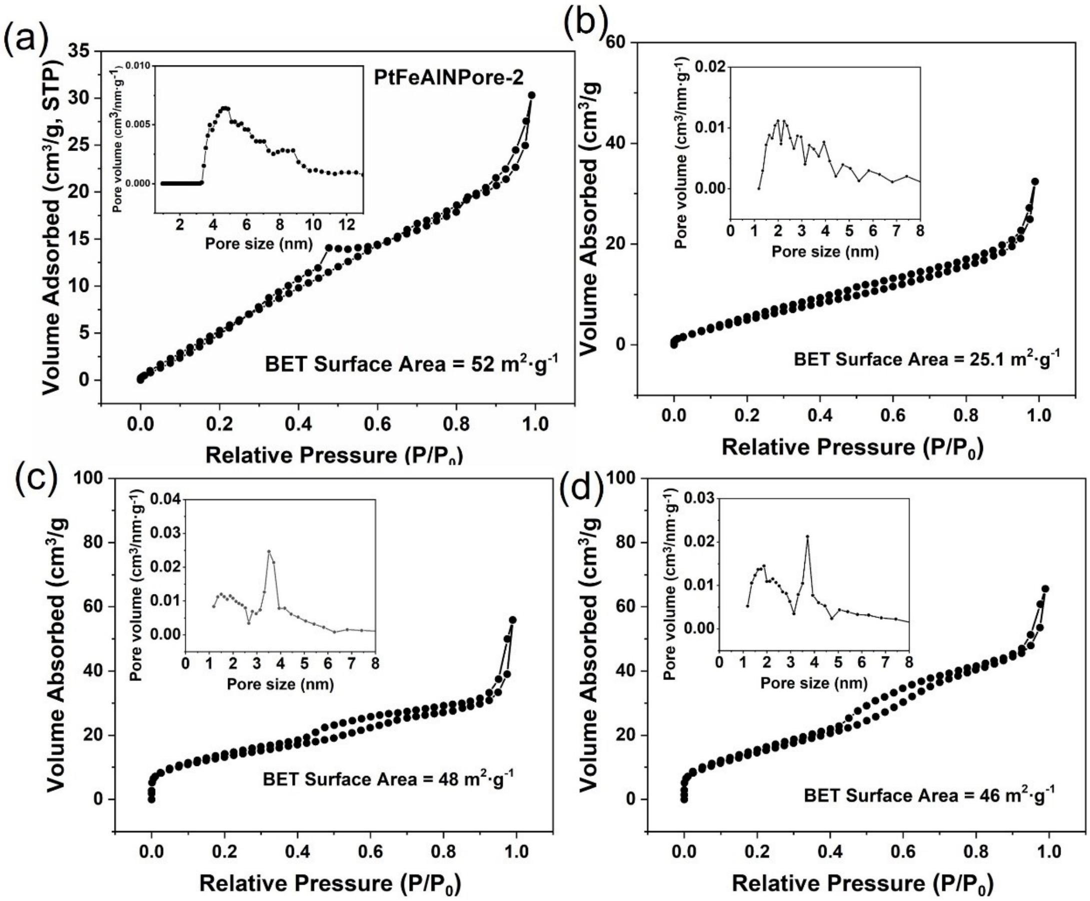

Figure 3. Nitrogen adsorption/desorption isotherm and corresponding size distribution curve of (a) PtFeAlNPore, (b) PtCoAlNPore, (c) PtNiAlNPore, (d) PtCuAlNPore.

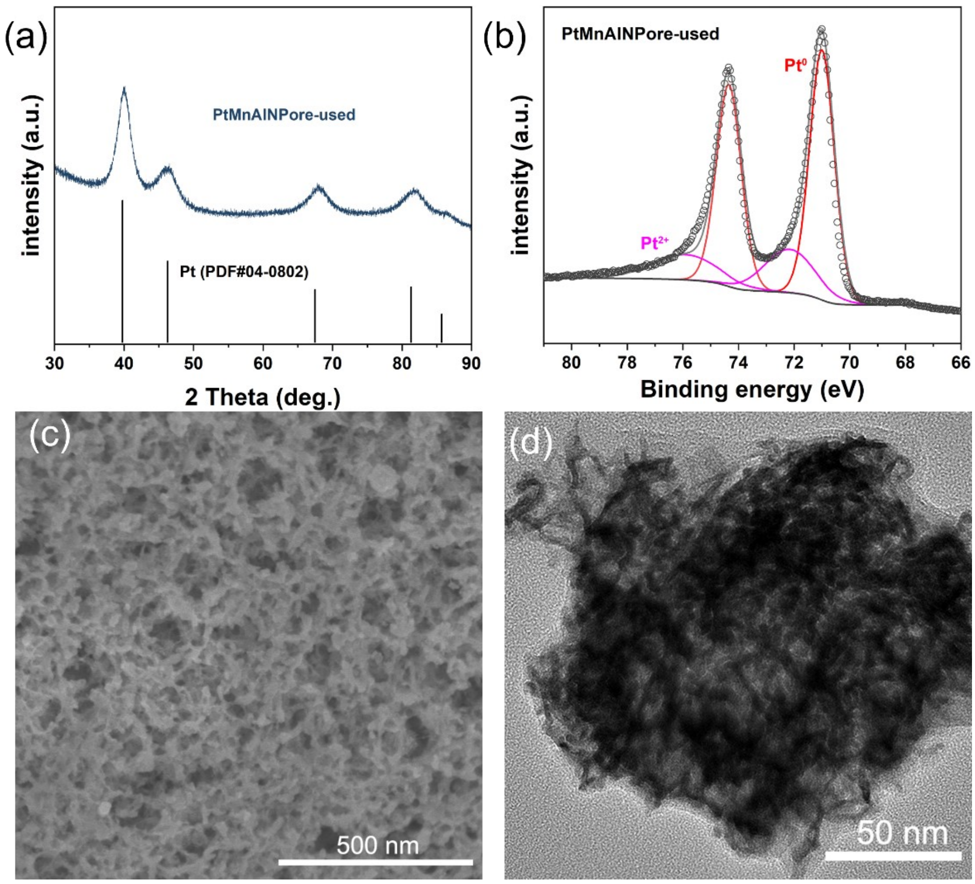

Figure 4. (a) XRD pattern, (b) Core-level XPS spectrum of Pt 4f, (c) SEM image, (d) TEM image of spent PtMnAlNPore.

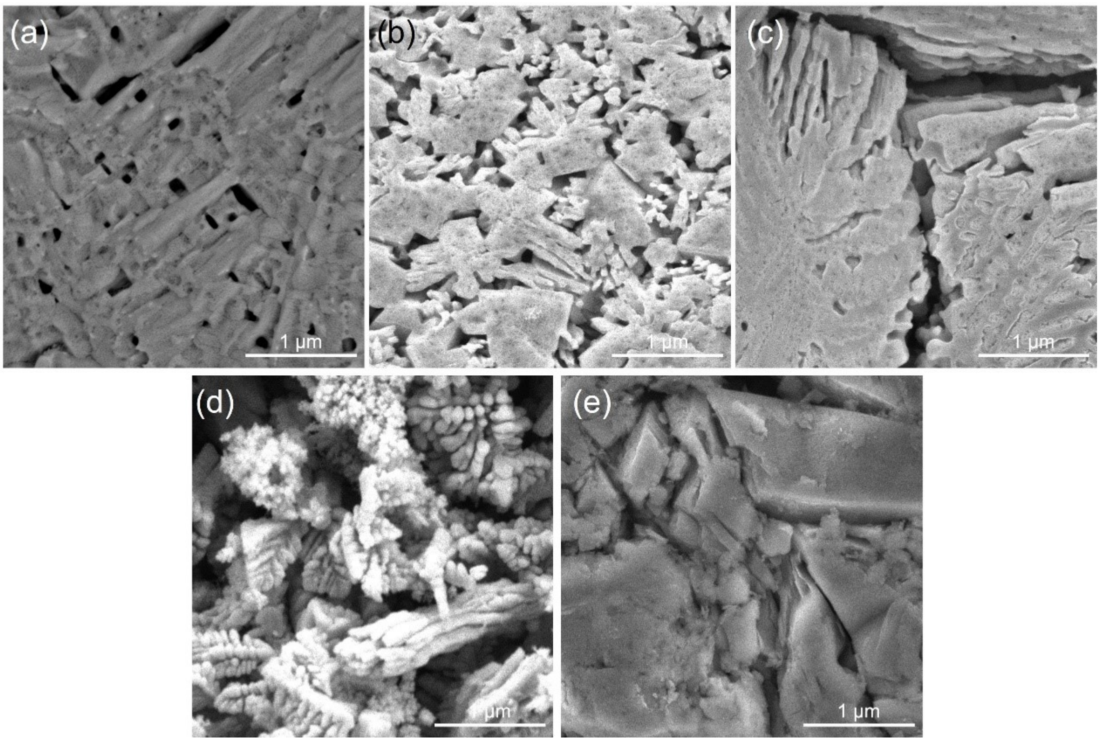

Figure 5. SEM image of once-dealloying samples (a) PtFeAlNPore, (b) PtCoAlNPore, (c) PtNiAlNPore, (d) PtCuAlNPore, (d) PtMnAlNPore.

Table S1. Comparison of catalysts for the hydrogenation of quinolines into py-THQs.

Catalyst	Temperature (°C)	H_2 pressure (MPa)	Yield of amine (%)	TOF (h^{-1})	Ref
PtMnAlNPore	60	0.3	92	376.5	This work
Pt@HA	140	2.0	97	65.36	[1]
Au_5Pt_1@SBA-15	25	1.0	92	35	[2]
1-rGO-NPs	70	1.5	100	39.6	[3]
Co_x@CN	120	3.0	100	4.1	[4]
PEG_{4000}	100	3.0	97	320	[5]
SA-Co/NSPC	120	2.0	99	-	[6]
$NiCl_2$/MIL-101(Cr)	150	5.0	93	-	[7]
Pt_{nano}	130	3.0	98	-	[8]
Ru-SiO_2@mSiO_2	130	3.0	100	-	[9]
Pd/NiO	120	5.0	93	-	[10]

Table S2. Atom ratio of ternary alloy catalysts.

PtMAlNPore (M= Fe, Co, Ni, Cu, and Mn)	Pt (%)	M (%)	Al (%)
PtFeAlNPore	69.3	20.3	10.4
PtCoAlNPore	72	14	14
PtNiAlNPore	68	18	14
PtCuAlNPore	72	15	13
PtMnAlNPore	85	7	8

4 Characterization data of products

Quinoline (1a)[11]

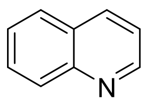

Colorless oil (53.9 mg, 81%). ^{1}H NMR (400 MHz, $CDCl_3$) δ 8.88 (dd, J = 4.2, 1.7 Hz, 1H), 8.19-8.00 (m, 2H), 7.75 (d, J = 8.2 Hz, 1H), 7.65-7.69 (m, 1H), 7.47-7.51 (m, 1H), 7.32 (dd, J = 8.3, 4.2 Hz, 1H). ^{13}C NMR (100 MHz, $CDCl_3$) δ 150.3, 148.2, 135.9, 129.4, 129.3, 128.2, 127.7, 126.4, 121.0, 77.4, 77.1, 76.8.

1,2,3,4-tetrahydroquinoline (2a)[12]

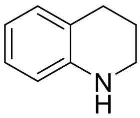

Yellow oil (53.9 mg, 81%). ^{1}H NMR (400 MHz, $CDCl_3$) δ 7.22-7.06 (m, 2H), 6.78 (td, J = 7.4, 1.1 Hz, 1H), 6.67-6.55 (m, 1H), 3.85 (br s, 1H), 3.48-3.33 (m, 2H), 2.92 (t, J = 6.4 Hz, 2H), 2.16-1.98 (m, 2H). ^{13}C NMR (100 MHz, $CDCl_3$) δ 144.7, 129.4, 126.6, 121.3, 116.7, 114.1, 77.4, 77.1, 76.8, 41.9, 26.9, 22.1.

2-methyl-1,2,3,4-tetrahydroquinoline (2b)[13]

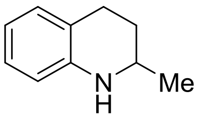

Yellow oil (58.9 mg, 80%). ^{1}H NMR (400 MHz, $CDCl_3$) δ 6.85-6.89 (m, 2H), 6.52 (t, J = 7.3 Hz, 1H), 6.37 (d, J = 8.3 Hz, 1H), 3.46 (br s, 1H), 3.28-3.32 (m, 1H), 2.74 (td, J = 14.0, 11.5, 5.5 Hz, 1H), 2.68 – 2.58 (m, 1H), 1.88 – 1.75 (m, 1H), 1.45-1.55 (m, 1H), 1.11 (d, J = 6.2 Hz, 3H). ^{13}C NMR (100 MHz, $CDCl_3$) δ 144.8, 129.3, 126.7, 121.2, 117.0, 114.1, 77.4, 77.1, 76.8, 47.2, 30.2, 26.7, 22.7.

4-methyl-1,2,3,4-tetrahydroquinoline (2c)[13]

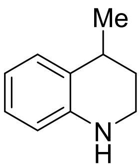

Yellow oil (61.1 mg, 83%). ^{1}H NMR (400 MHz, $CDCl_3$) δ 7.05 (d, J = 7.5 Hz, 1H), 6.96 (t, J = 7.4 Hz, 1H), 6.63 (t, J = 7.4 Hz, 1H), 6.47 (d, J = 7.9 Hz, 1H), 3.58 (br s, 1H), 3.22-3.35 (m, 2H), 2.87-2.95 (m, 1H), 1.98 (ddt, J = 13.1, 9.0, 5.1 Hz, 1H), 1.67 (dtd, J = 12.9, 6.4, 3.6 Hz, 1H), 1.28 (d, J = 7.0 Hz, 3H). ^{13}C NMR (100 MHz, $CDCl_3$) δ 144.23, 128.50, 126.78, 126.71, 117.06, 114.27, 77.43, 77.12, 76.80, 39.08, 30.29, 29.93, 22.71.

8-methyl-1,2,3,4-tetrahydroquinoline (2d)[14]

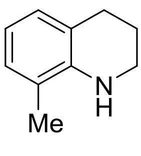

Colorless oil (62.6 mg, 83%). ^{1}H NMR (400 MHz, $CDCl_3$) δ 6.77 (dd, J = 10.6, 7.7 Hz, 2H), 6.46 (t, J = 7.4 Hz, 1H), 3.27 (t, J = 5.6 Hz, 2H), 2.69 (t, J = 6.4 Hz, 2H), 1.98 (s, 3H), 1.81-1.87 (m, 2H). ^{13}C NMR (100 MHz, $CDCl_3$) δ 142.7, 127.9, 127.4, 121.2, 120.9, 116.5, 77.4, 77.1, 76.8, 42.4, 27.4, 22.2, 17.2.

6-methoxy-1,2,3,4-tetrahydroquinoline (2e)[15]

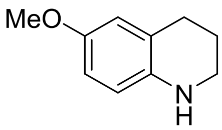

Colorless oil (68.5 mg, 84%). ^1H NMR (400 MHz, $CDCl_3$) δ 6.58-6.42 (m, 2H), 6.35 (d, J = 8.5 Hz, 1H), 3.63 (s, 3H), 3.33 (br s, 1H), 3.21-3.09 (m, 2H), 2.65 (t, J = 6.5 Hz, 2H), 1.83 (dt, J = 11.9, 6.5 Hz, 2H). ^{13}C NMR (100 MHz, $CDCl_3$) δ 151.9, 138.9, 122.9, 115.6, 114.9, 112.9, 77.5, 77.1, 76.8, 55.8, 42.4, 27.2, 22.5.

8-hydroxy-1,2,3,4-tetrahydroquinolin (2f)[16]

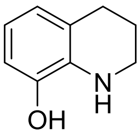

White solid (40.3 mg, 54%). M.P. 118-119 °C. ^1H NMR (400 MHz, $CDCl_3$) δ 6.50-6.42 (m, 3H), 4.62 (s, 2H), 3.20 (s, 2H), 2.67 (s, 2H), 1.85 (s, 2H). ^{13}C NMR (100 MHz, $CDCl_3$) δ 143.4, 133.3, 123.6, 121.8, 117.4, 112.6, 77.4, 77.1, 76.8, 41.7, 26.6, 22.2.

1,2,3,4-tetrahydroquinolin-8-amine (2g)[17]

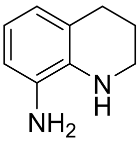

Brown oil (45.2 mg, 61%). ^1H NMR (400 MHz, $CDCl_3$) δ6.52-6.44 (m, 3H), 3.21 (br s, 5H), 2.68 (t, J = 6.3 Hz, 2H), 1.85-1.79 (m, 2H). ^{13}C NMR (100 MHz, $CDCl_3$) δ 133.9, 133.78, 123.3, 121.1, 118.1, 114.1, 77.4, 77.1, 76.8, 42.6, 27.0, 22.4.

6-chloro-1,2,3,4-tetrahydroquinoline (2h)[12]

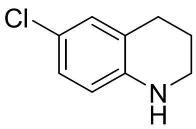

Yellow oil (62.9 mg, 75%). ^1H NMR (400 MHz, $CDCl_3$) δ6.90-6.88 (m, 2H), 6.37 (d, J = 8.2 Hz, 1H), 3.32-3.19 (m, 2H), 2.71 (t, J = 6.4 Hz, 2H), 1.96-1.82 (m, 2H). ^{13}C NMR (100 MHz, $CDCl_3$) δ 143.3, 129.1, 126.6, 123.0, 121.3, 115.2, 77.4, 77.1, 76.8, 41.9, 26.9, 21.8.

7-chloro-2-methyl-1,2,3,4-tetrahydroquinoline (2i)[18]

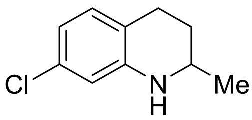

Yellow oil (65.4 mg, 72%). ^1H NMR (400 MHz, $CDCl_3$) δ 6.85 (d, J = 8.0 Hz, 1H), 6.54 (dd, *J* = 8.0, 2.1 Hz, 1H), 6.44 (d, *J* = 2.0 Hz, 1H), 3.76 (br s, 1H), 3.39 (dqd, *J* = 9.3, 6.3, 3.0 Hz, 1H), 2.86-2.60 (m, 2H), 2.01-1.86 (m, 1H), 1.55 (dddd, *J* = 12.9, 11.1, 9.9, 5.5 Hz, 1H), 1.21 (d, *J* = 6.3 Hz, 3H). ^{13}C NMR (100 MHz, $CDCl_3$) δ 145.8, 132.0, 130.2, 119.4, 116.7, 113.3, 77.4, 77.1, 76.8, 47.1, 29.8, 26.2, 22.5.

methyl 1,2,3,4-tetrahydroquinoline-6-carboxylate (2j)[19]

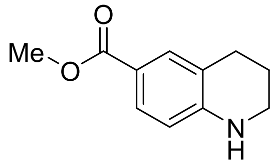

Colorless oil (76.5 mg, 80%). ^{1}H NMR (400 MHz, $CDCl_3$) δ 7.62-7.64 (m, 2H), 6.37 (d, *J* = 9.0 Hz, 1H), 4.29 (br s, 1H), 3.82 (s, 3H), 3.37-3.24 (m, 2H), 2.73 (t, *J* = 6.2 Hz, 2H), 1.97-1.81 (m, 2H). ^{13}C NMR (100 MHz, $CDCl_3$) δ 167.6, 148.9, 131.2, 129.1, 119.8, 117.1, 112.6, 77.4, 77.1, 76.8, 51.4, 41.6, 26.9, 21.3.

5 Copies of ^{1}H and ^{13}C NMR spectra of products

^{1}H NMR, 400 MHz, $CDCl_3$

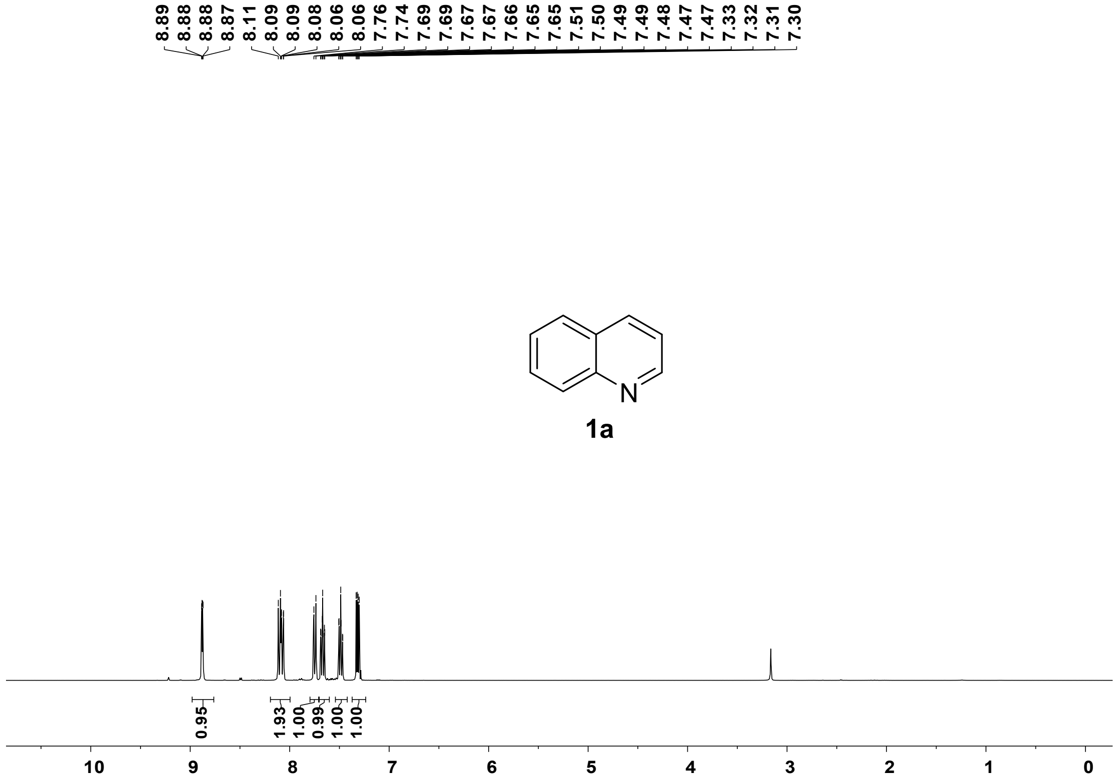

^{13}C NMR, 100 MHz, $CDCl_3$

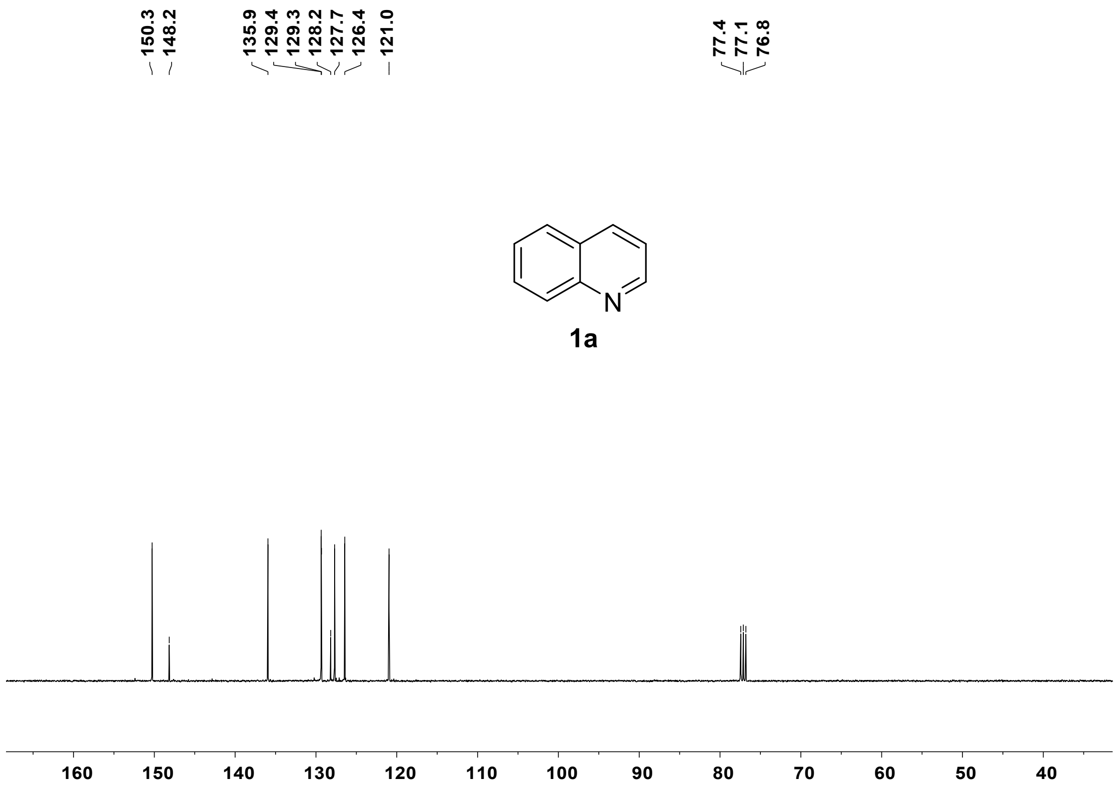

^{1}H NMR, 400 MHz, $CDCl_3$

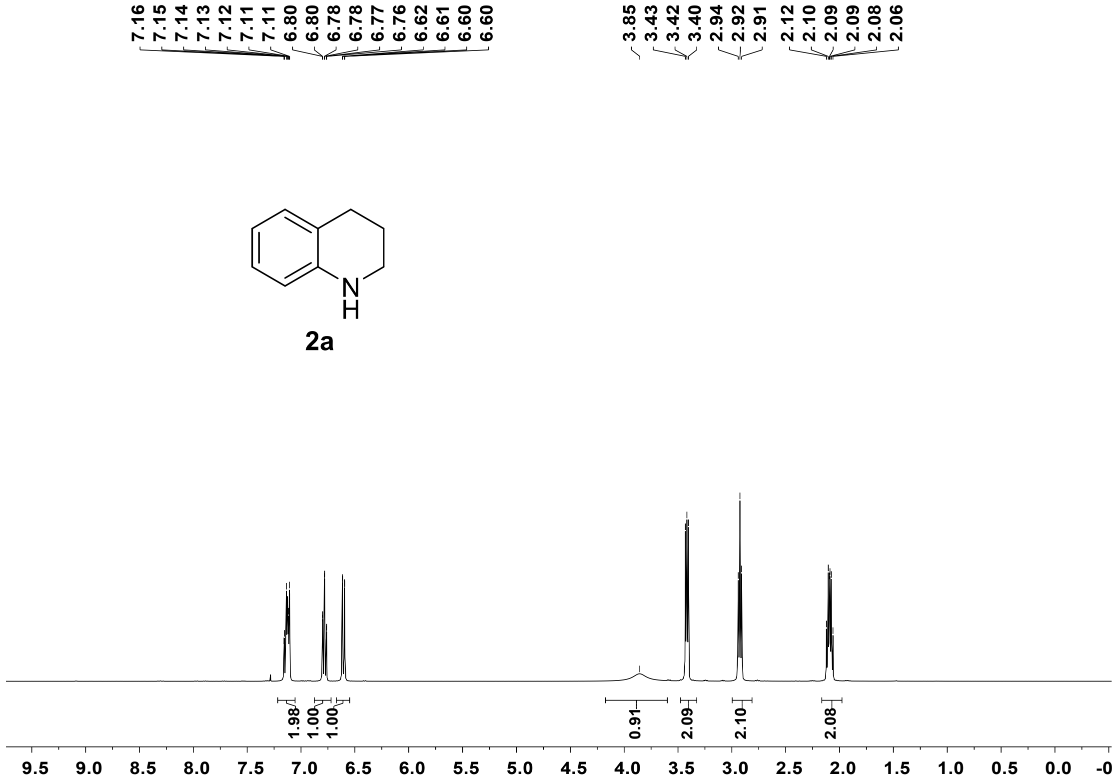

^{13}C NMR, 100 MHz, $CDCl_3$

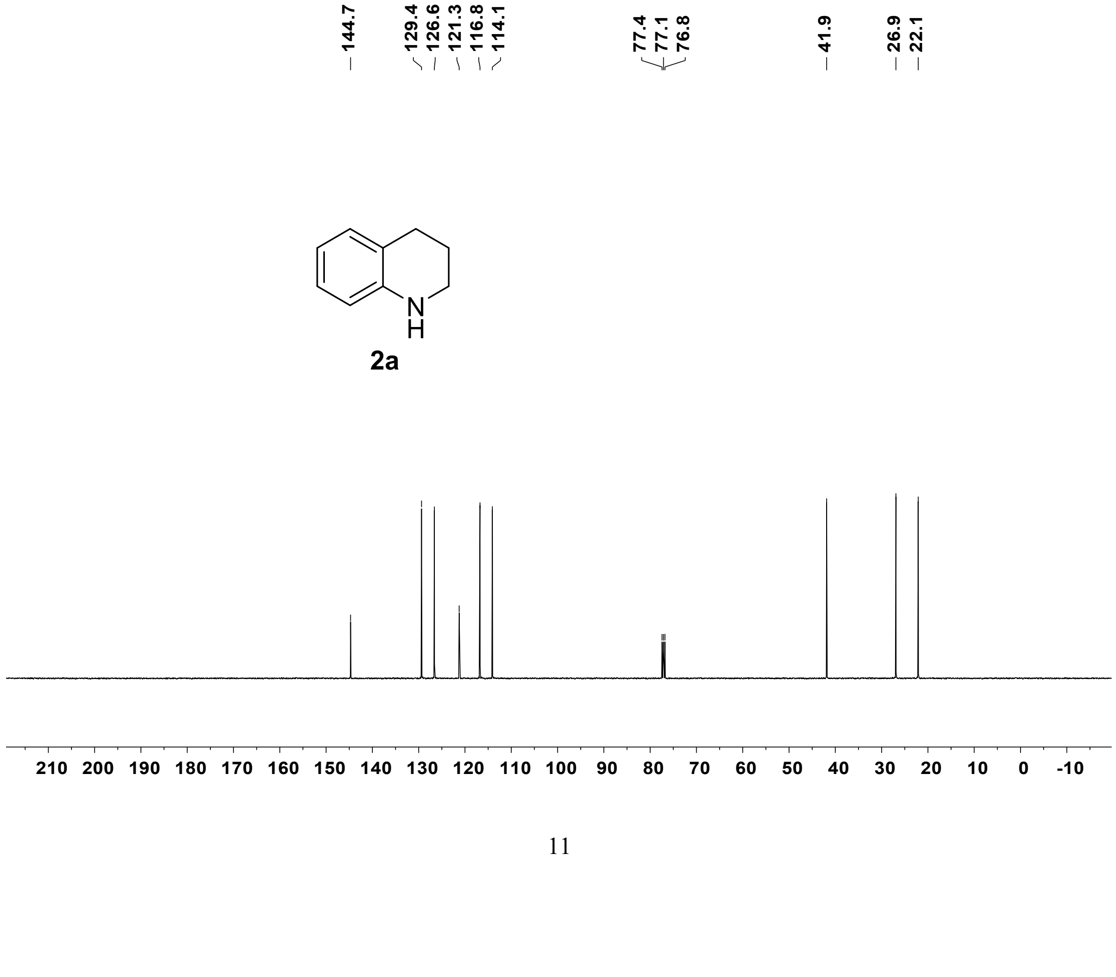

^{1}H NMR, 400 MHz, $CDCl_3$

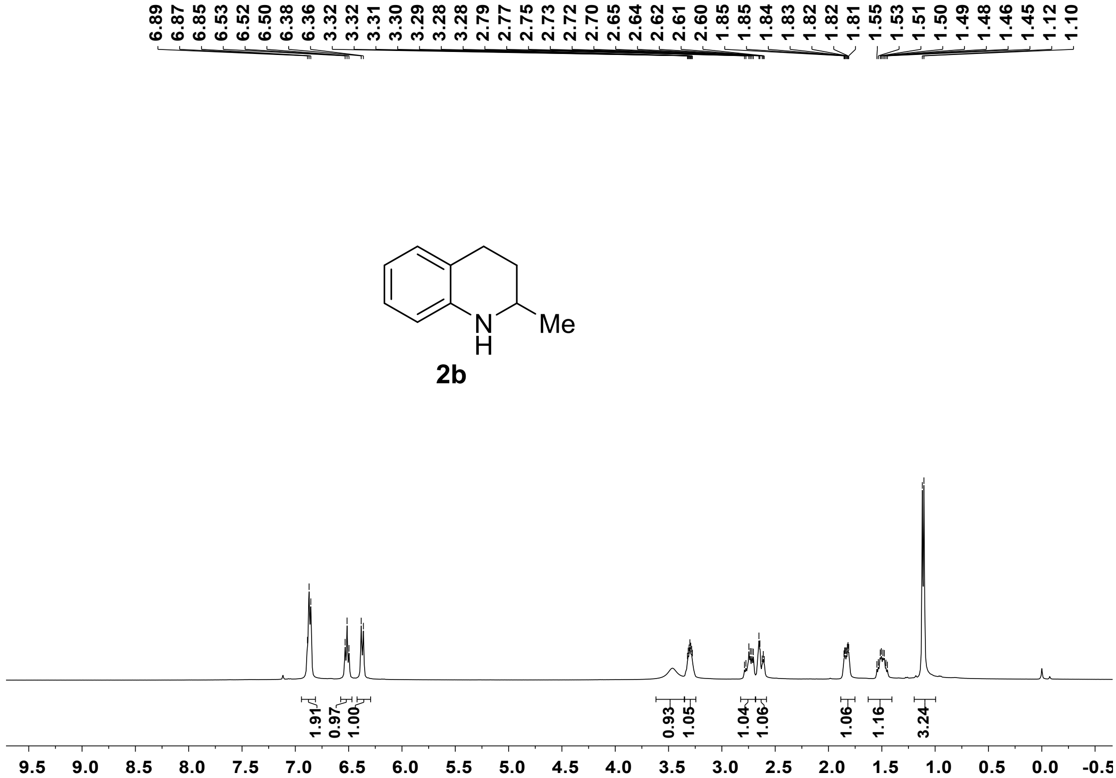

2b

^{13}C NMR, 100 MHz, $CDCl_3$

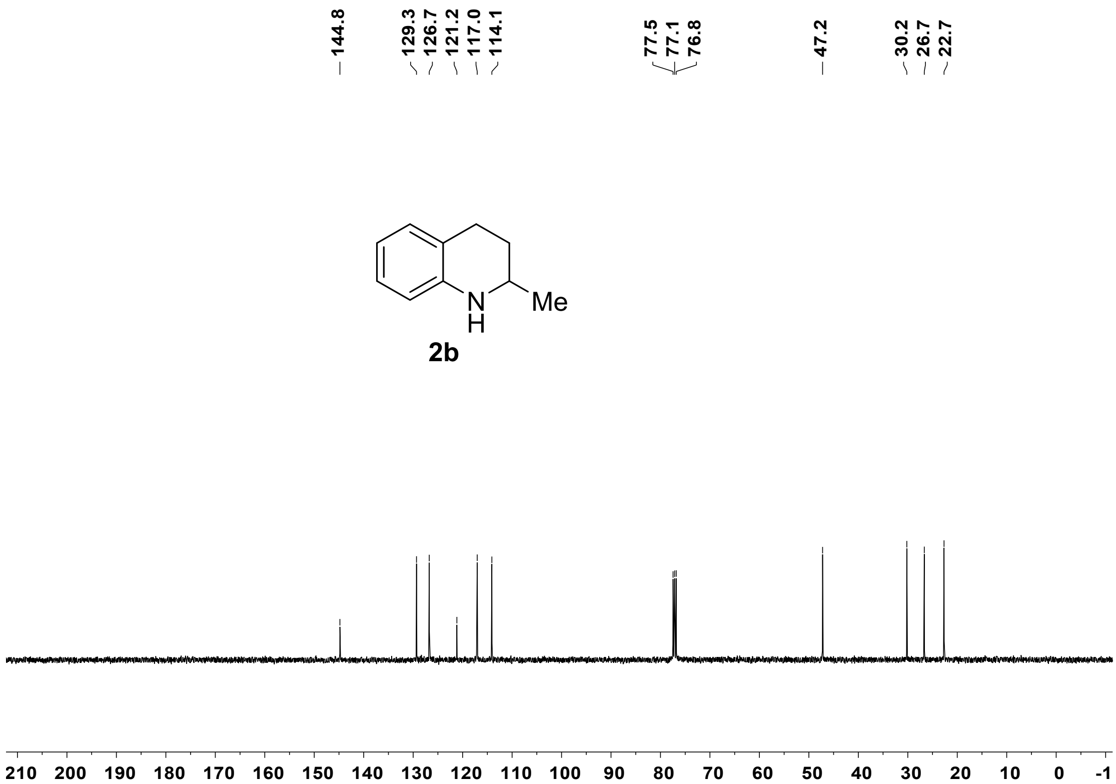

2b

[1]H NMR, 400 MHz, $CDCl_3$

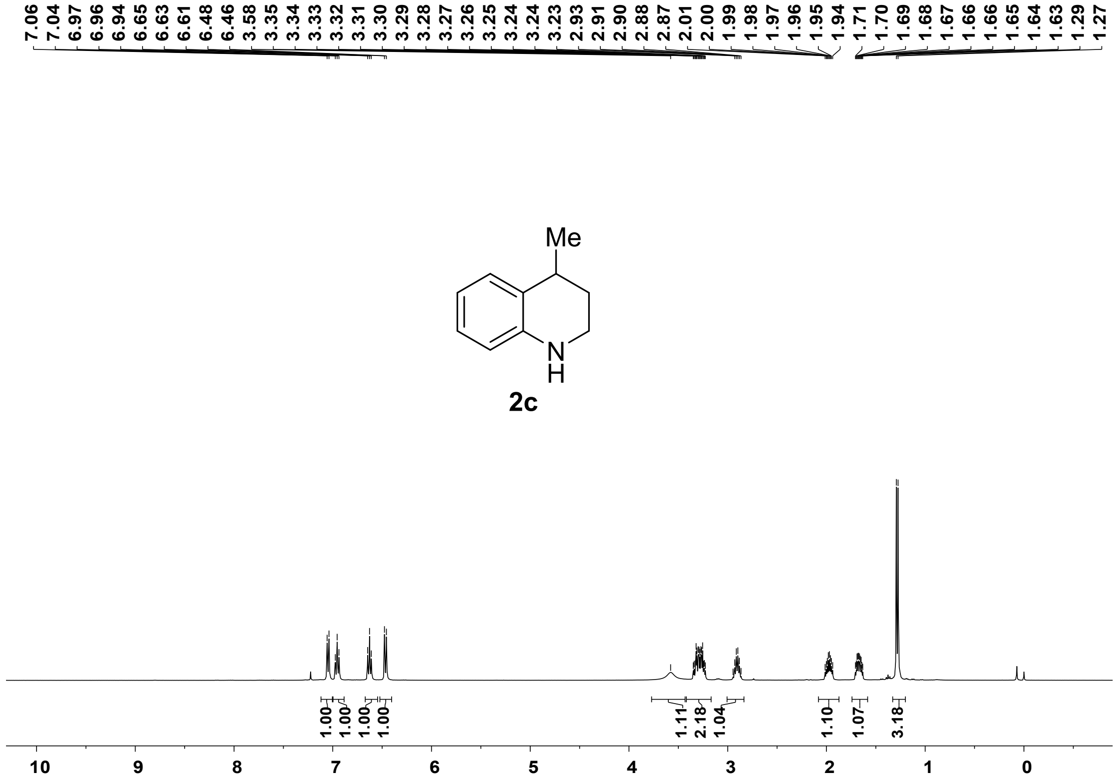

[13]C NMR, 100 MHz, $CDCl_3$

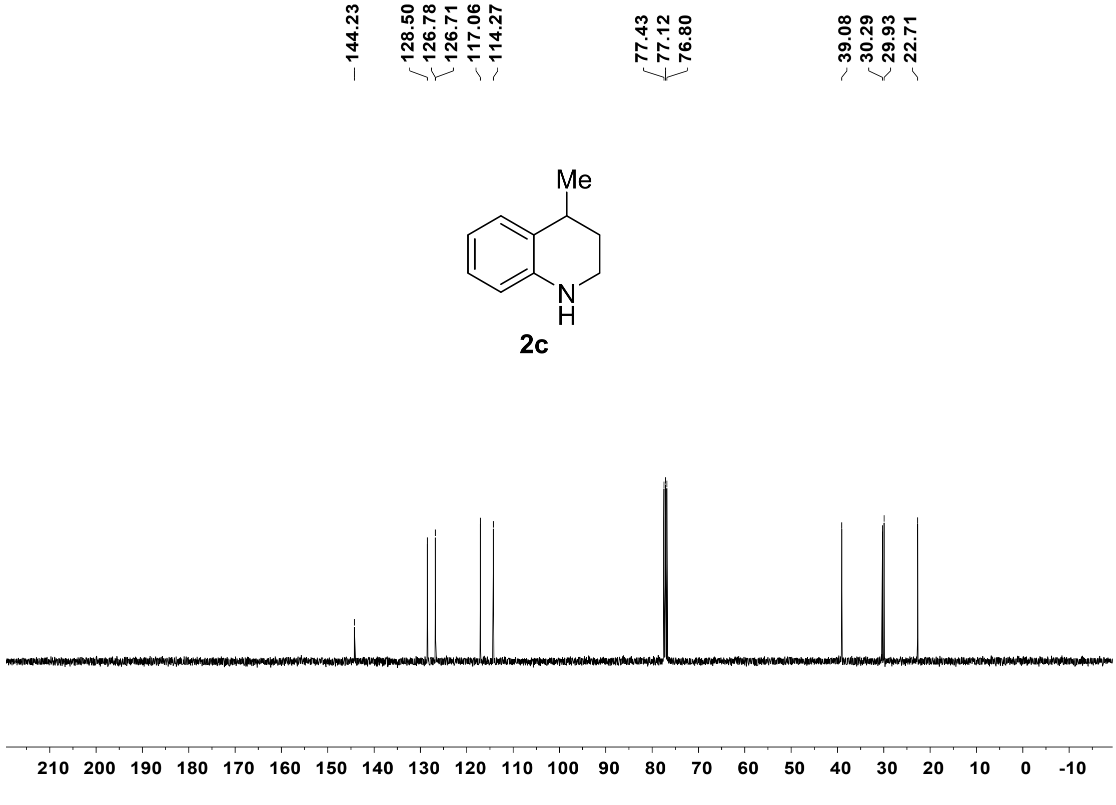

^{1}H NMR, 400 MHz, $CDCl_3$

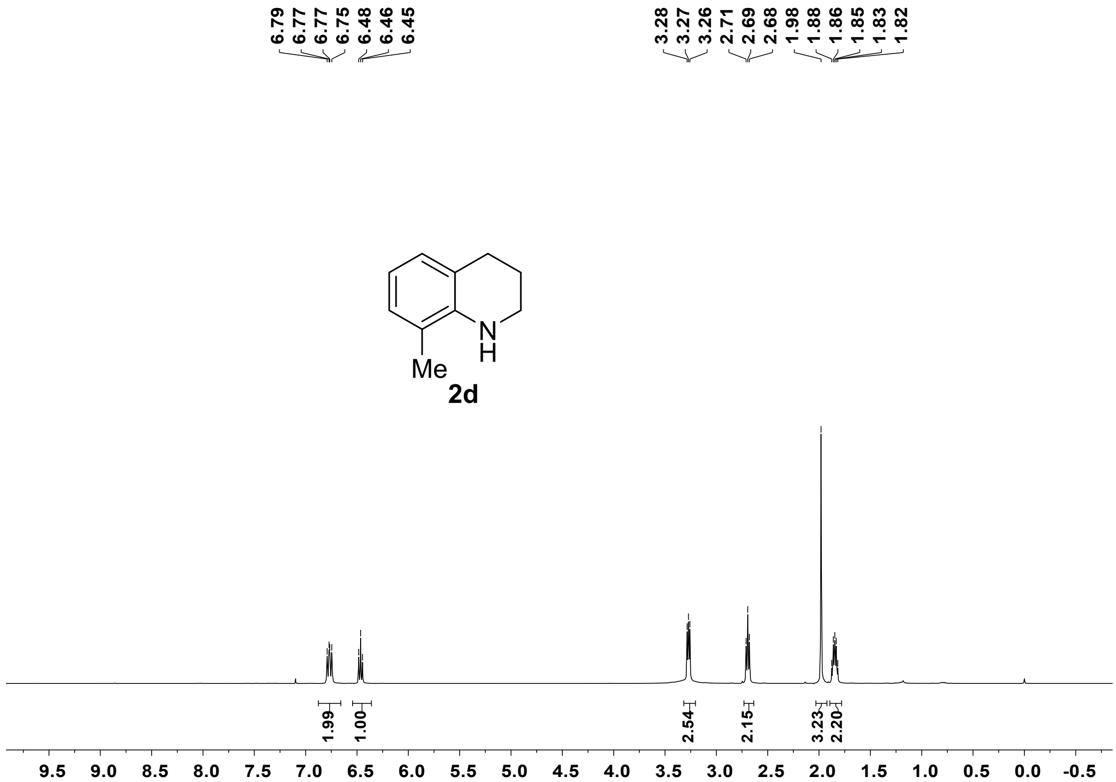

^{13}C NMR, 100 MHz, $CDCl_3$

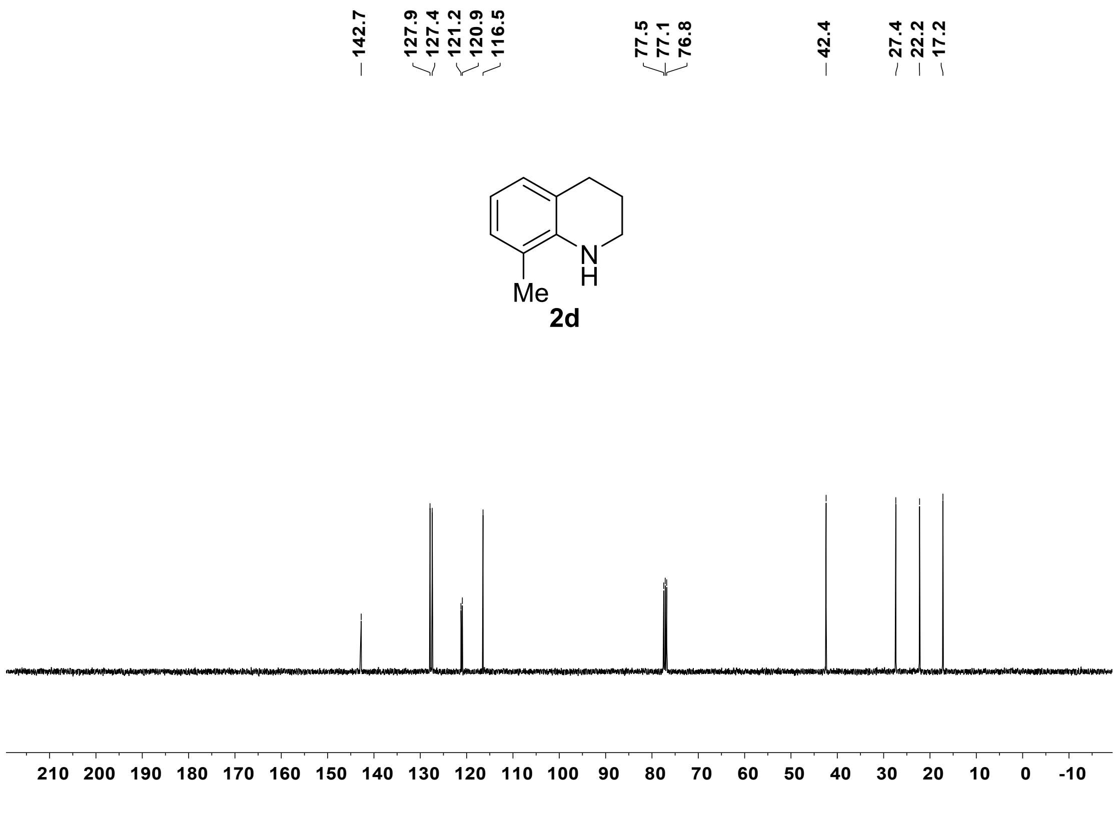

^{1}H NMR, 400 MHz, $CDCl_3$

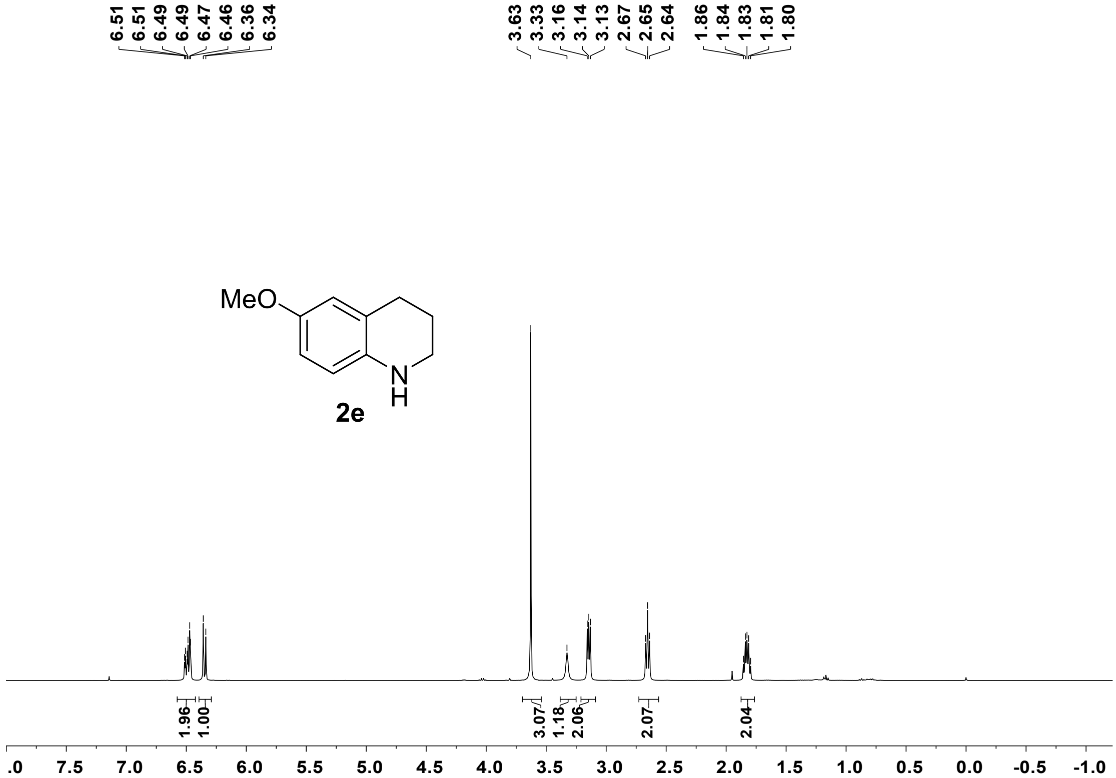

^{13}C NMR, 100 MHz, $CDCl_3$

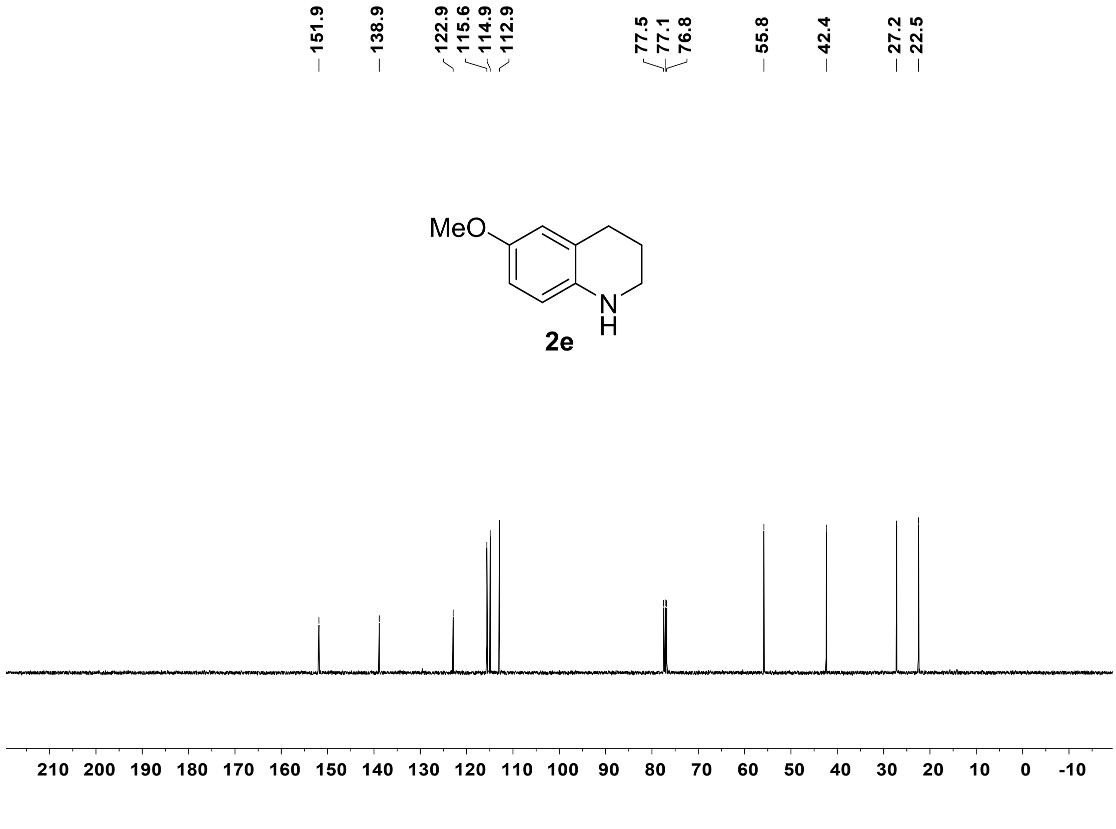

^{1}H NMR, 400 MHz, $CDCl_3$

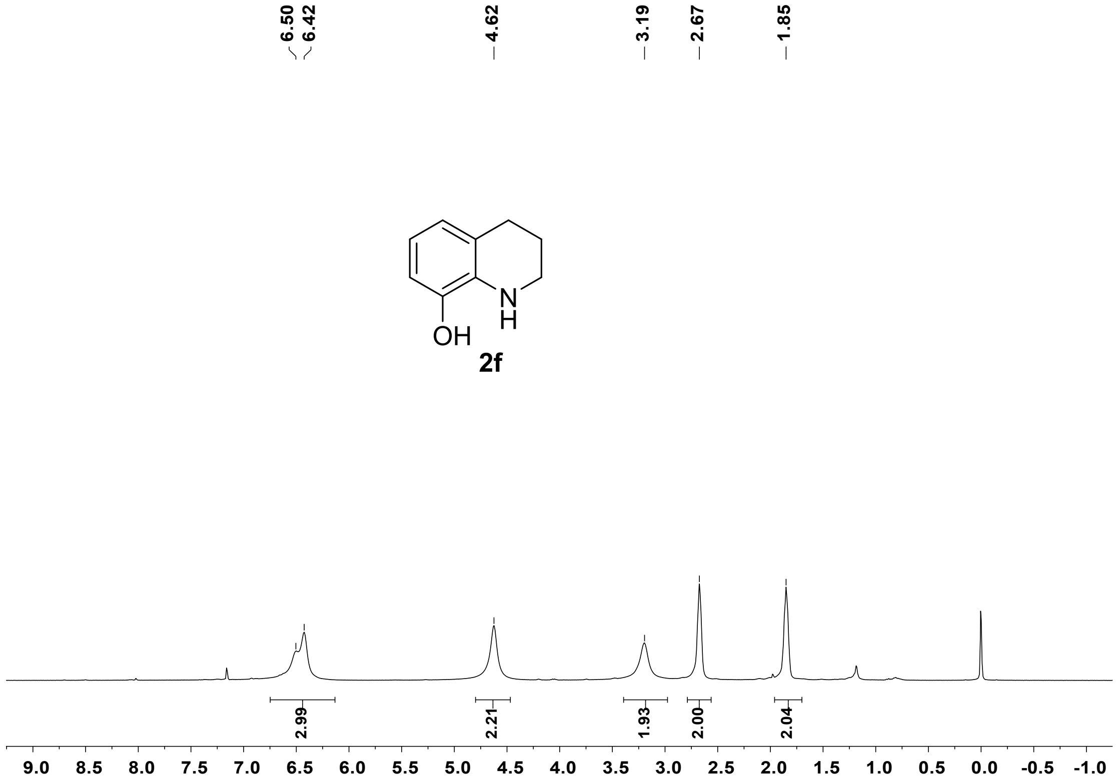

^{13}C NMR, 100 MHz, $CDCl_3$

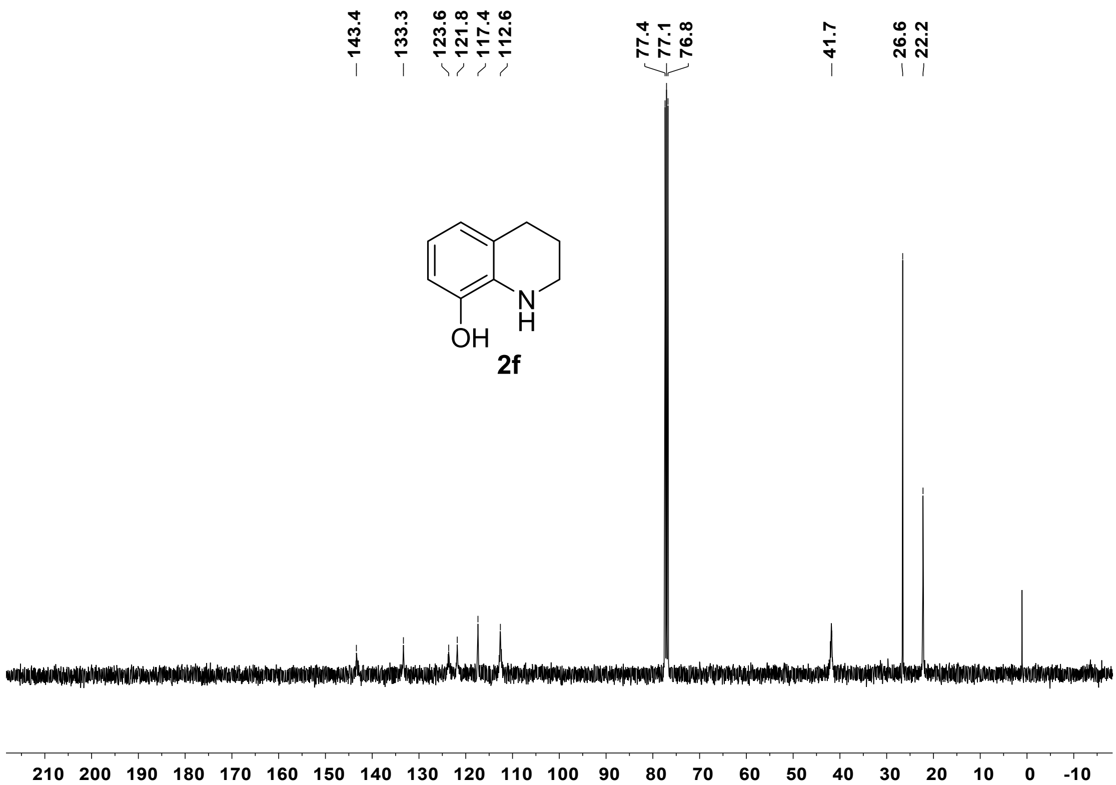

^{1}H NMR, 400 MHz, $CDCl_3$

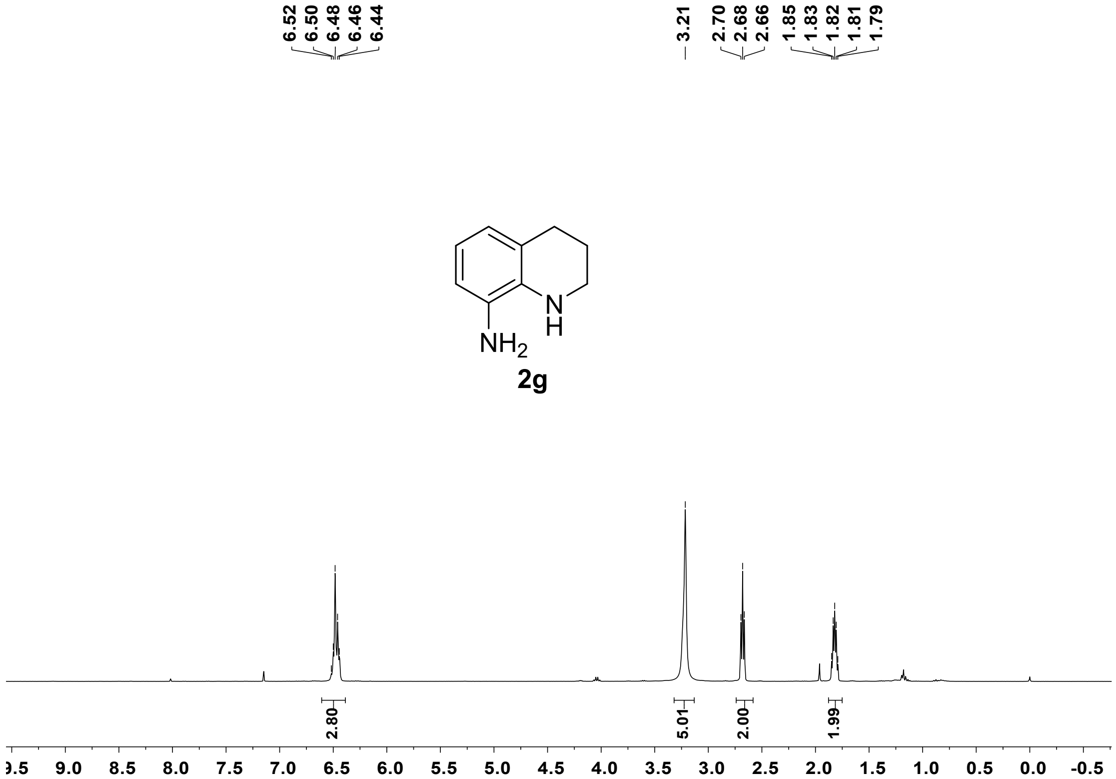

^{13}C NMR, 100 MHz, $CDCl_3$

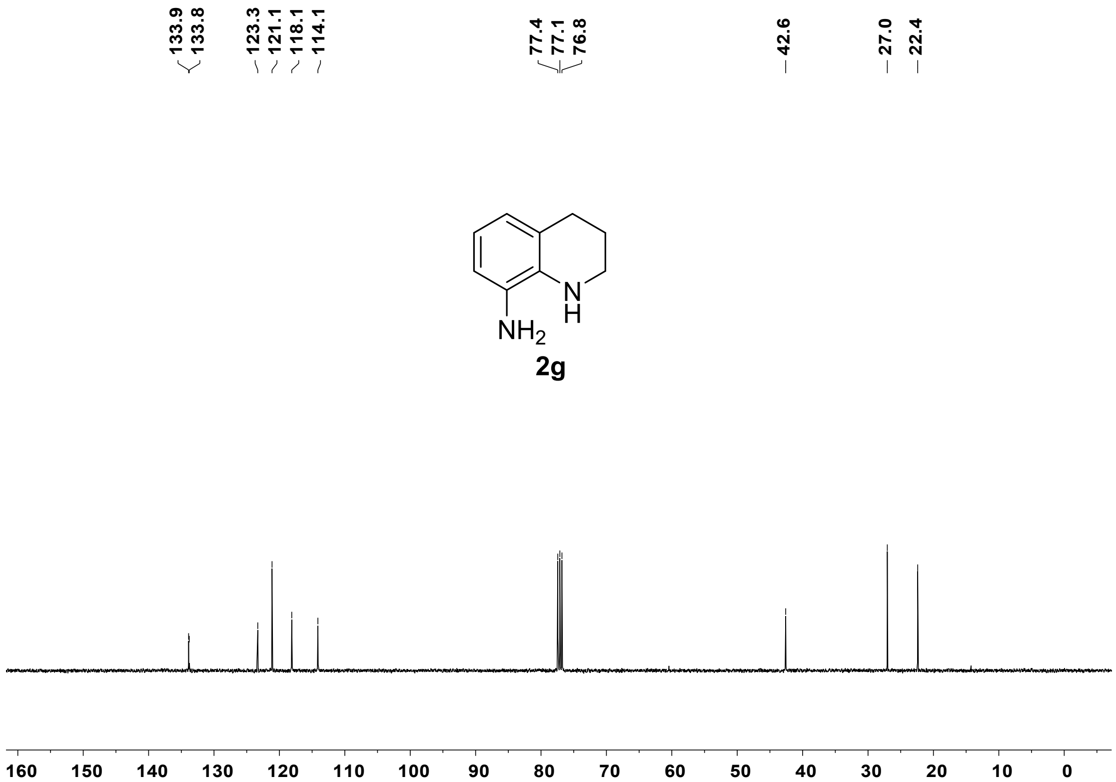

^1H NMR, 400 MHz, $CDCl_3$

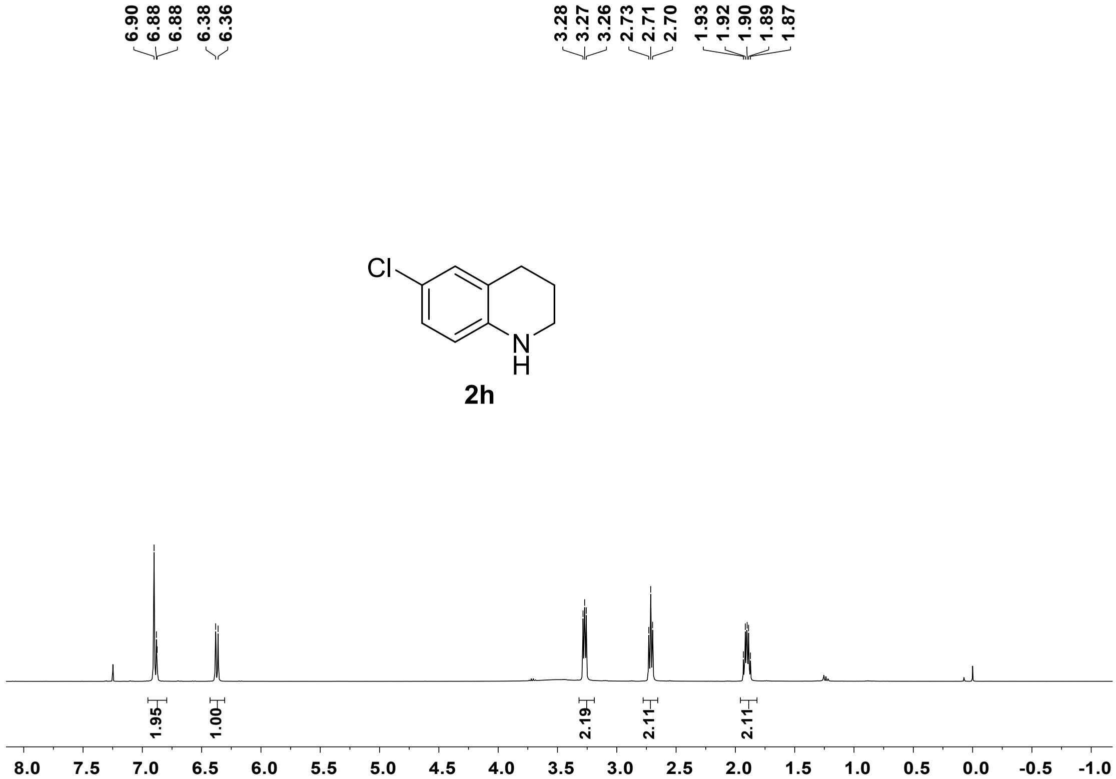

^{13}C NMR, 100 MHz, $CDCl_3$

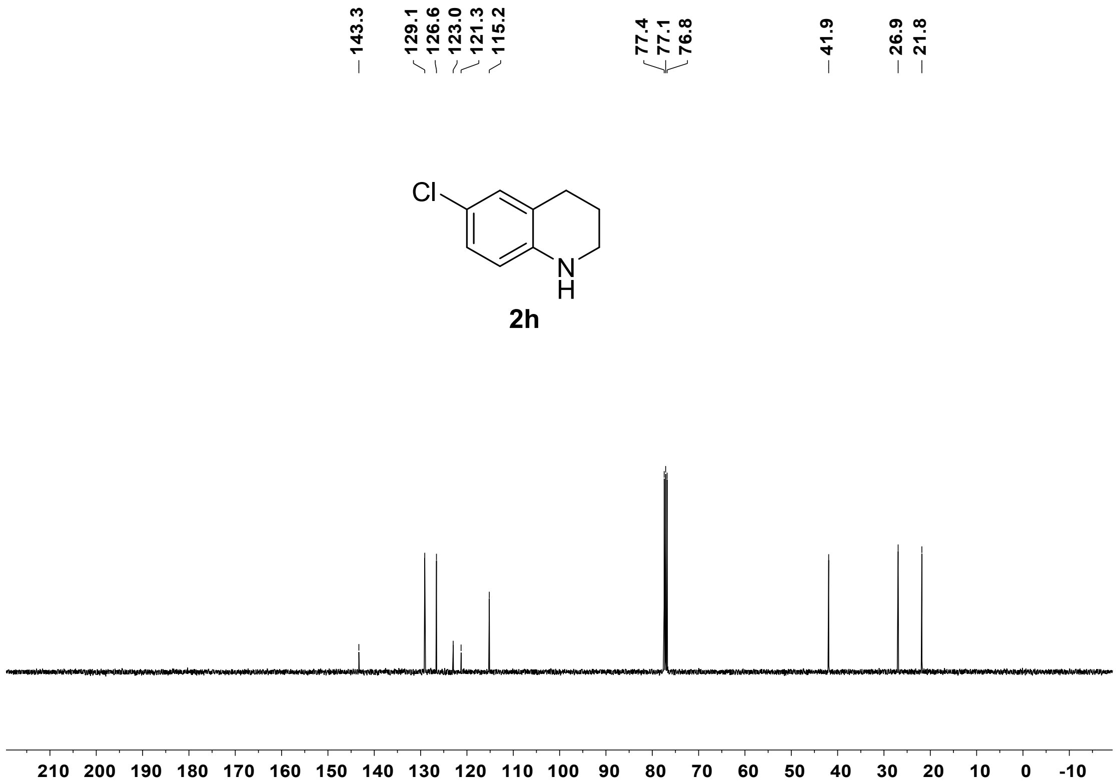

^{1}H NMR, 400 MHz, $CDCl_3$

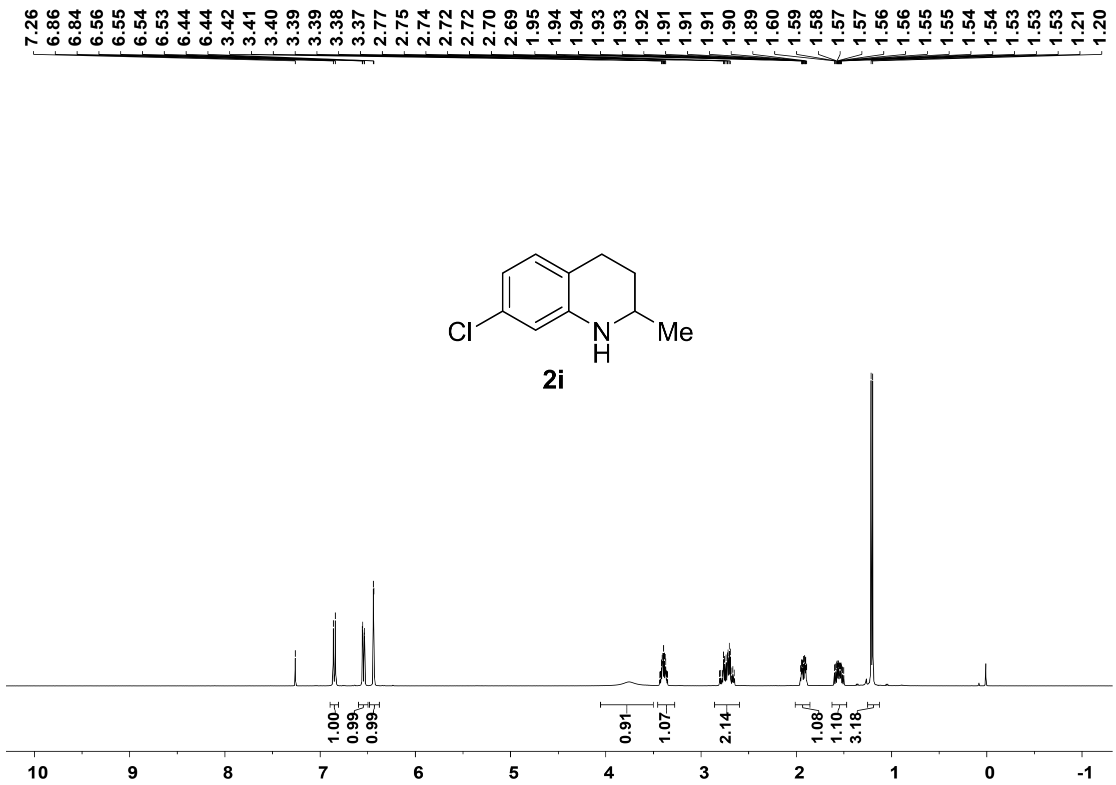

^{13}C NMR, 100 MHz, $CDCl_3$

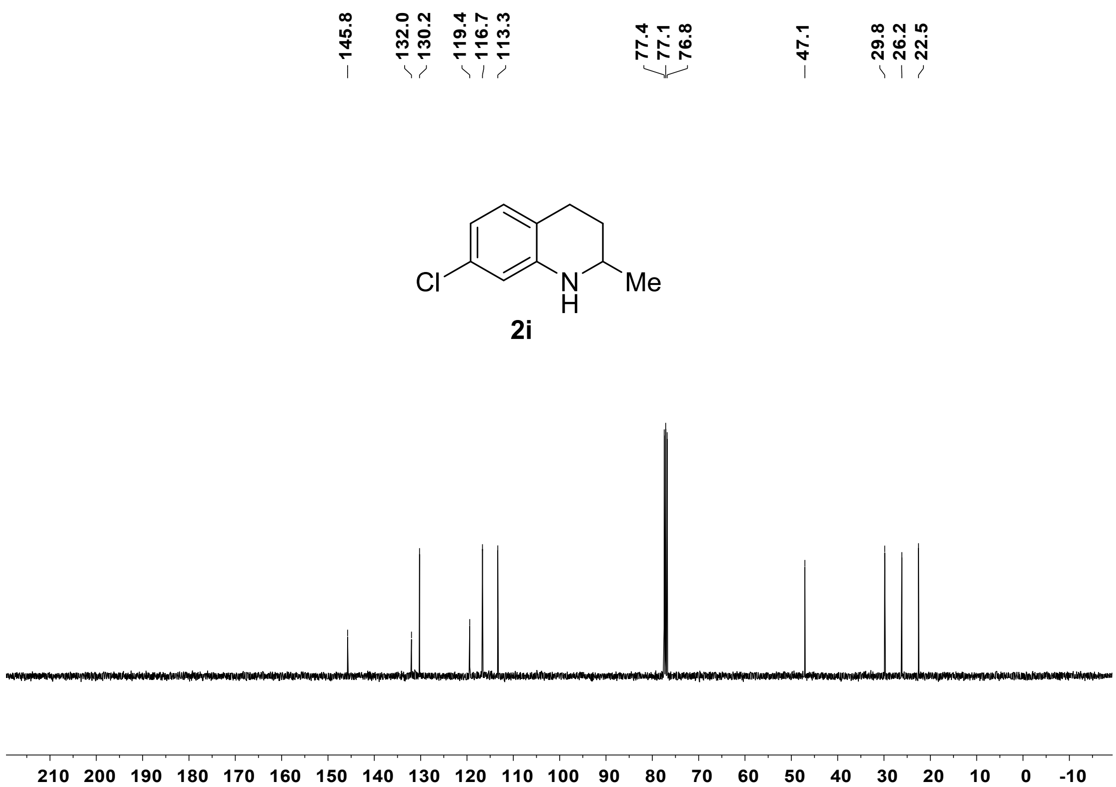

^{1}H NMR, 400 MHz, $CDCl_3$

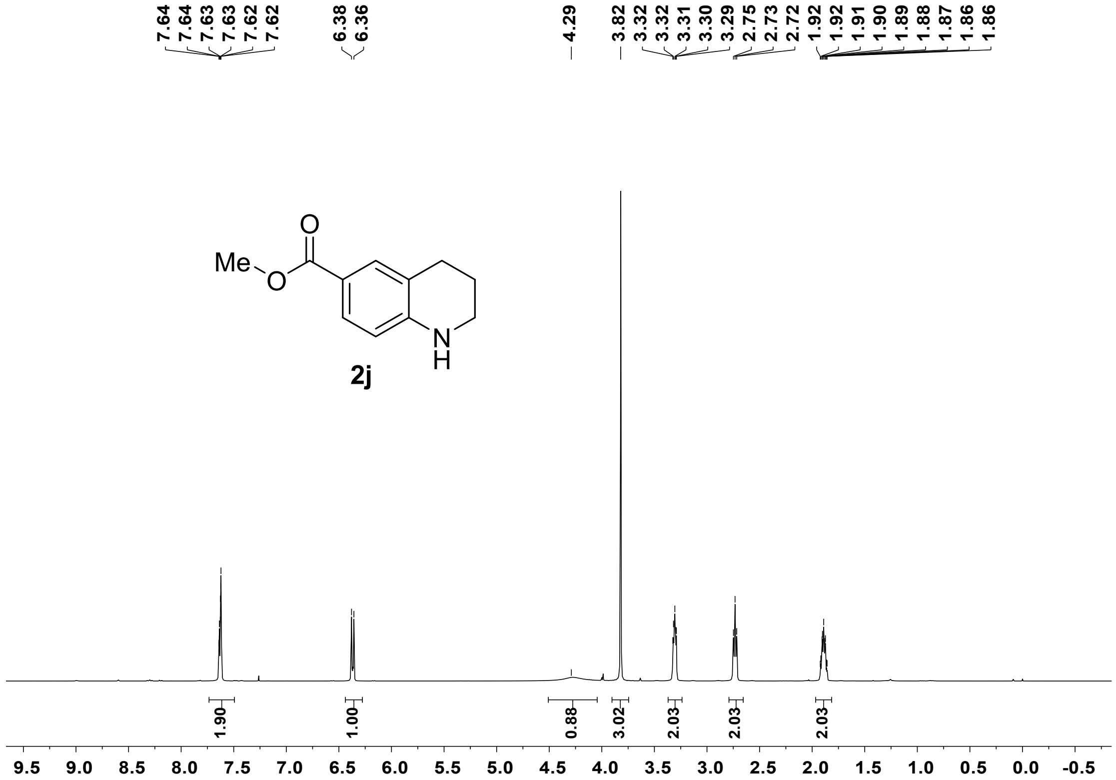

^{13}C NMR, 100 MHz, $CDCl_3$

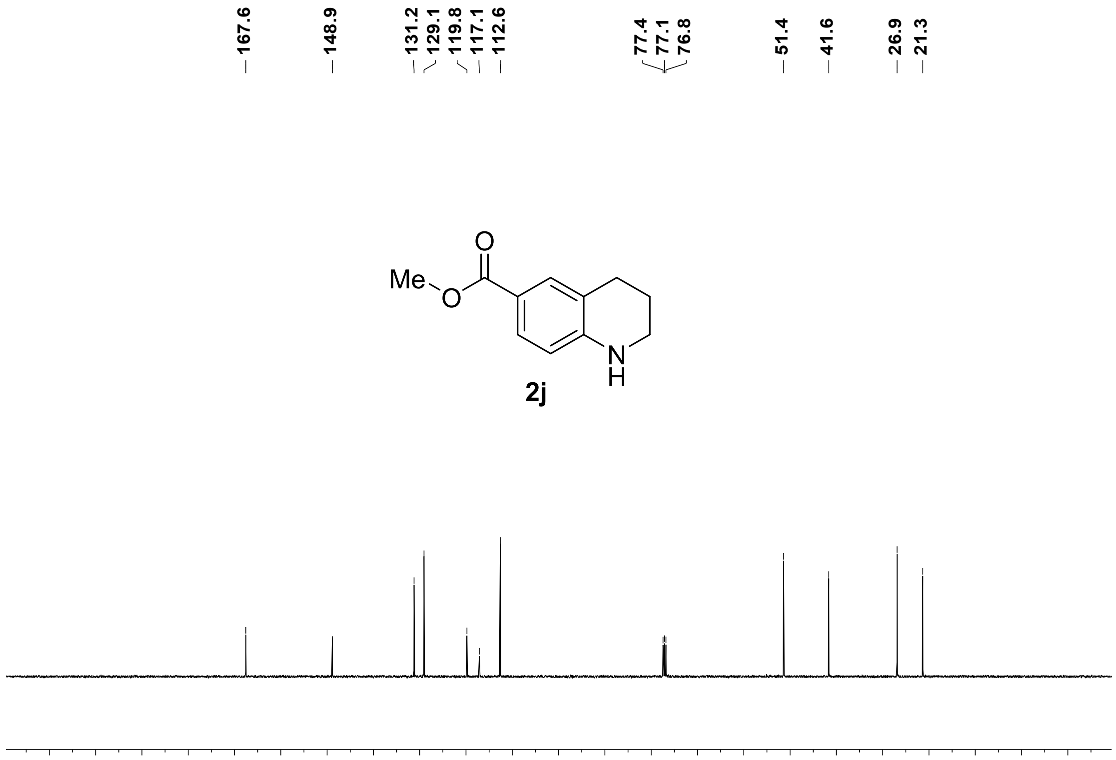

6 Reference

[1] Y. Tan, M. Han, P. Peng, Z. Sun, J. Shi, Y. Huang, J. Chen, L. Bai, J. Yang, Q. Chen, Strengthening spillover hydrogenation of quinoline compounds over platinum-encapsulated amorphized HA zeolite catalyst, Molecular Catalysis 545 (2023). https://doi.org/10.1016/j.mcat.2023.113210.

[2] J. Zhao, H. Yuan, G. Yang, Y. Liu, X. Qin, Z. Chen, C. Weng-Chon, L. Zhou, S. Fang, AuPt bimetallic nanoalloys supported on SBA-15: A superior catalyst for quinoline selective hydrogenation in water, Nano Research 15(3) (2021) 1796-1802. https://doi.org/10.1007/s12274-021-3732-1.

[3] A. Mollar-Cuni, S. Martín, G. Guisado-Barrios, J.A. Mata, Dual role of graphene as support of ligand-stabilized palladium nanoparticles and carbocatalyst for (de)hydrogenation of N-heterocycles, Carbon 206 (2023) 314-324. https://doi.org/10.1016/j.carbon.2023.02.014.

[4] Z. Wei, Y. Chen, J. Wang, D. Su, M. Tang, S. Mao, Y. Wang, Cobalt Encapsulated in N-Doped Graphene Layers: An Efficient and Stable Catalyst for Hydrogenation of Quinoline Compounds, ACS Catal. 6(9) (2016) 5816-5822. https://doi.org/10.1021/acscatal.6b01240.

[5] M. Niu, Y. Wang, P. Chen, D. Du, J. Jiang, Z. Jin, Highly efficient and recyclable rhodium nanoparticle catalysts for hydrogenation of quinoline and its derivatives, Catalysis Science & Technology 5(10) (2015) 4746-4749. https://doi.org/10.1039/C5CY00940E.

[6] F. Tang, G. Zhang, L. Wang, J. Huang, Y.-N. Liu, Unsymmetrically N, S-coordinated single-atom cobalt with electron redistribution for catalytic hydrogenation of quinolines, J. Catal. 414 (2022) 101-108. https://doi.org/https://doi.org/10.1016/j.jcat.2022.08.033.

[7] V.M. Asaula, A.S. Lytvynenko, A.M. Mishura, M.M. Kurmach, V.V. Buryanov, K.S. Gavrilenko, S.V. Ryabukhin, D.M. Volochnyuk, S.V. Kolotilov, In-situ formation of NixB/MIL-101(Cr) and Pd/MIL-101(Cr) composites for catalytic hydrogenation of quinoline, Inorg. Chem. Commun. 121 (2020) 108203. https://doi.org/https://doi.org/10.1016/j.inoche.2020.108203.

[8] X. Xue, M. Zeng, Y. Wang, Highly active and recyclable Pt nanocatalyst for hydrogenation of quinolines and isoquinolines, Appl. Catal., A. 560 (2018) 37-41. https://doi.org/https://doi.org/10.1016/j.apcata.2018.04.039.

[9] L. Zhang, X. Wang, Y. Xue, X. Zeng, H. Chen, R. Li, S. Wang, Cooperation between the surface hydroxyl groups of Ru–SiO2@mSiO2 and water for good catalytic performance for hydrogenation of quinoline, Catalysis Science & Technology 4(7) (2014) 1939-1948. https://doi.org/10.1039/C3CY01071F.

[10] Y. Wang, X. Cui, Y. Deng, F. Shi, Catalytic hydrogenation of aromatic rings catalyzed by Pd/NiO, RSC Advances 4(6) (2014) 2729-2732. https://doi.org/10.1039/C3RA45600E.

[11] J.C.A. Flanagan, L.M. Dornan, M.G. McLaughlin, N.G. McCreanor, M.J. Cook, M.J. Muldoon, The synthesis of N-heterocycles via copper/TEMPO catalysed aerobic oxidation of amino alcohols, Green Chemistry 14(5) (2012) 1281-1283. https://doi.org/10.1039/C2GC35062A.

[12] L. Zhang, D. Xie, S. Zhang, A Method for the Synthesis of 1,2,3,4-Tetrahydroquinolines through Reduction of Quinolin-2(1H)-ones Promoted by SmI2/H2O/Et3N, Eur. J. Org. Chem. 2022(47) (2022) e202201063. https://doi.org/https://doi.org/10.1002/ejoc.202201063.

[13] Y. Liang, J. Luo, Y. Diskin-Posner, D. Milstein, Designing New Magnesium Pincer Complexes for Catalytic Hydrogenation of Imines and N-Heteroarenes: H2 and N–H Activation by Metal–Ligand Cooperation as Key Steps, Journal of the American Chemical Society 145(16) (2023) 9164-9175. https://doi.org/10.1021/jacs.3c01091.

[14] M. Yan, T. Jin, Q. Chen, H.E. Ho, T. Fujita, L.-Y. Chen, M. Bao, M.-W. Chen, N. Asao, Y.

Yamamoto, Unsupported Nanoporous Gold Catalyst for Highly Selective Hydrogenation of Quinolines, Org. Lett. 15(7) (2013) 1484-1487. https://doi.org/10.1021/ol400229z.

[15] Y.-G. Ji, K. Wei, T. Liu, L. Wu, W.-H. Zhang, “Naked” Iridium(IV) Oxide Nanoparticles as Expedient and Robust Catalysts for Hydrogenation of Nitrogen Heterocycles: Remarkable Vicinal Substitution Effect and Recyclability, Adv. Synth. Catal. 359(6) (2017) 933-940. https://doi.org/https://doi.org/10.1002/adsc.201601370.

[16] J. Wu, J.H. Barnard, Y. Zhang, D. Talwar, C.M. Robertson, J. Xiao, Robust cyclometallated Ir(iii) catalysts for the homogeneous hydrogenation of N-heterocycles under mild conditions, Chem. Commun. 49(63) (2013) 7052-7054. https://doi.org/10.1039/C3CC44567D.

[17] D. Bhattacharyya, S. Nandi, P. Adhikari, B.K. Sarmah, M. Konwar, A. Das, Boric acid catalyzed chemoselective reduction of quinolines, ORG BIOMOL CHEM 18(6) (2020) 1214-1220. https://doi.org/10.1039/C9OB02673H.

[18] Y.-N. Duan, X. Du, Z. Cui, Y. Zeng, Y. Liu, T. Yang, J. Wen, X. Zhang, Homogeneous Hydrogenation with a Cobalt/Tetraphosphine Catalyst: A Superior Hydride Donor for Polar Double Bonds and N-Heteroarenes, Journal of the American Chemical Society 141(51) (2019) 20424-20433. https://doi.org/10.1021/jacs.9b11070.

[19] T. Bhatt, K. Natte, Transfer Hydrogenation of N- and O-Containing Heterocycles Including Pyridines with H3N–BH3 Under the Catalysis of the Homogeneous Ruthenium Precatalyst, Org. Lett. 26(4) (2024) 866-871. https://doi.org/10.1021/acs.orglett.3c04051.